*Journal of Sound and Vibration*, **262**(2) (2003) pp. 333-345

# Multiple chatter frequencies in milling processes

Insperger, T.

PhD student
Department of Applied Mechanics
Budapest University of Technology
and Economics
Budapest, H-1521, Hungary
Phone: +36 1 463 1332
Fax: +36 1 463 3471
e-mail: inspi@mm.bme.hu

Stépán, G. *

Professor, Head of Department
Department of Applied Mechanics
Budapest University of Technology
and Economics
Budapest, H-1521, Hungary
Phone: +36 1 463 1369
Fax: +36 1 463 3471
e-mail: stepan@mm.bme.hu

Bayly, P. V.

Associate Professor
Department of Mechanical Engineering
Washington University
1 Brookings Drive
St. Louis, MO 63130
Phone: (314)-935-6081
Fax: (314)-935-4014
e-mail: pvb@mecf.wustl.edu

Mann, B. P.

PhD student
Department of Mechanical Engineering
Washington University
1 Brookings Drive
St. Louis, MO 63130
Phone: (314)-935-7562
Fax: (314)-935-4014
e-mail: bpm1@cec.wustl.edu

**Abstract**

Analytical and experimental identifications of the chatter frequencies in milling processes are presented. In the case of milling, there are several frequency sets arising from the vibration signals, as opposed to the single well-defined chatter frequency of the unstable turning process. Frequency diagrams are constructed analytically and attached to the stability charts of mechanical models of high-speed milling. The corresponding quasiperiodic solutions of the governing time-periodic delay-differential equations are also identified with some milling experiments in the case of highly intermittent cutting.

**Keywords:** tooth pass excitation, high-speed milling, time delay, Floquet theory

# 1 Introduction

The history of machine tool chatter goes back to almost 100 years, when Taylor [1] described machine tool chatter as the most obscure and delicate of all problems facing the machinist. After the extensive work of Tlusty *et al.* [2] and Tobias [3], the so-called

*all correspondence to this author

regenerative effect has become the most commonly accepted explanation for machine tool chatter [4-7]. This effect is related to the cutting force variation due to the wavy workpiece surface cut during the previous revolution. The corresponding mathematical models are delay-differential equations (DDE). Stability properties can be predicted through the investigation of these DDEs [8, 9]. The identification of the arising vibrations can effectively be supported by frequency analysis of the chatter signal [10-12]. The stability charts published in the specialist literature are almost always accompanied by frequency diagrams that represent the chatter frequencies at the loss of stability. The reason of this custom is that these frequencies can precisely be identified experimentally and so this is a direct way to verify theoretical models and predictions.

For the simplest model of turning, the governing equation of motion is an autonomous DDE with a corresponding infinite dimensional state space. This fact implies the existence of an infinite number of characteristic roots, most of them having negative real parts referring to damped components of the vibration signals. There may be some finite number of characteristic roots that have positive real parts. Each of those roots which are pure imaginary correspond to a single well defined vibration frequency. For turning, these critical chatter frequencies are usually 0–15% above the well separated lowest (or single) natural frequency of the machine tool structure [8]. The study of nonlinear phenomena in the cutting process showed that these chatter frequencies are related to unstable periodic motions about stable stationary cutting, i.e. a so-called subcritical Hopf bifurcation occurs, as it was proved experimentally by Shi and Tobias [13] and analytically by Stépán and Kalmár-Nagy [14].

The model of the milling process is more complex. The tooth pass excitation effect results in a parametric excitation of the system, and the governing equation of motion is a time periodic DDE. These systems can be investigated by the extended Floquet theory of DDEs [15-17]. A time periodic DDE has an infinite dimensional state space, too, but characteristic multipliers are defined instead of characteristic roots. Most of the infinite number of characteristic multipliers are located within the open unit disc of the complex plane referring to damped oscillation components, and only a finite number of multipliers can have a magnitude greater than 1. The critical multipliers are located on the unit circle and each of them refers to an infinite series of vibration frequencies.

Several analytical methods were developed to determine the stability properties of the milling process [18-23]. Numerical simulation may also serve a satisfactory result for this purpose [24, 25]. The analytical investigations lead to the realization of new bifurcation phenomena. In addition to Hopf bifurcation, period doubling bifurcation is also a typical way of stability loss in milling processes, as it was shown analytically by Davies *et al.* [21], Insperger and Stépán [26], Corpus and Endres [27], Bayly *et al.* [22] and experimentally by Davies *et al.* [21], Bayly *et al.* [22]. The nonlinear analysis of Stépán and Szalai [28] showed that this period doubling bifurcation is subcritical.

In spite of all these research efforts, the identification of the critical chatter frequencies at the loss of stability is not a trivial task either experimentally or theoretically. The power spectra of the signals show several peaks of complicated structure. Some of them refer to the tooth pass excitation effect, others refer to the regenerative effect and the natural frequency of the tool also appears. In the subsequent sections, a clear picture is given about these frequencies arising in chatter during the milling process.

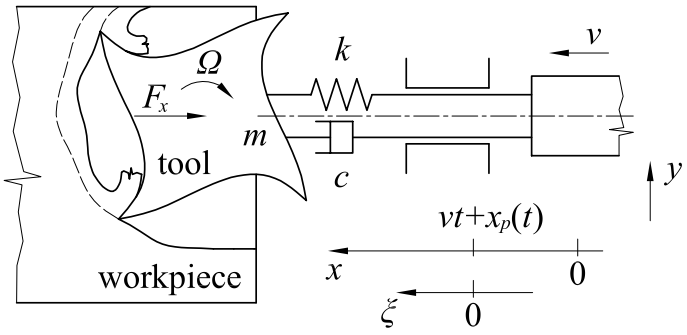


Figure 1: Regenerative mechanical model for milling

## 2 Mechanical model

The mechanical model of the milling process can be seen in Figure 1. The mass $m$ of the tool, the damping coefficient $c$ and the spring stiffness $k$ can be determined via the modal analysis of the machine tool. $x$ is the displacement of the centre of the tool relative to the workpiece. The structure is assumed to be flexible in the $x$ direction only. This reduces the model to single degree of freedom (SDOF). This SDOF model is appropriate, for example, when a thin-walled workpiece is the most flexible part of the structure. In this case, the workpiece is likely to be asymmetric and compliant in one direction while rigid in the orthogonal direction.

Assume the prescribed feed motion to be uniform with a constant speed $v$ of the tool. According to Newton's law, the equation of motion reads

$$m\ddot{x}(t) = -F_x + k(vt - x(t)) + c(v - \dot{x}(t))\,. \tag{1}$$

To determine the cutting force $F_x$, further analysis of the cutting process is needed. The tangential component of the cutting force acting on an active tooth (number $j$) can be approximated by

$$F_{j\,t} = Kw(f \sin\varphi_j)^{x_F}\,, \tag{2}$$

where $K$ is the cutting coefficient, $w$ is the depth of cut, $f$ is the feed per tooth and $\varphi_j$ denotes the angular position of the tool. The exponent $x_F$ is a small constant. $x_F = 0.8$ is a typical value for this parameter [29]. The normal component of the cutting force is usually estimated as [29]

$$F_{j\,n} = 0.3\,F_{j\,t}\,. \tag{3}$$

Recently, Halley [30] also verified this formula experimentally. The $x$ component of the cutting force depends on the angular position of the tool as it can be seen in Figure 2

$$F_{j\,x} = g_j(t)\,(F_{j\,t}\cos\varphi_j + F_{j\,n}\sin\varphi_j)\,. \tag{4}$$

Here, $g_j(t)$ is a screen function [31], it is equal to 1, if the $j$th tooth is active and 0 if it is not.

Let us denote the spindle speed of the tool by $\Omega$ [rpm], so the tooth pass period is $\tau = 60/(z\Omega)$ [s], where $z$ is the number of the teeth. The feed is equal to the difference of the present and the delayed position of the tool, i.e., $f = x(t) - x(t-\tau)$. The angular position of each tooth depends on the time as follows $\varphi_j = \Omega t + j\vartheta$, where $\vartheta = 2\pi/z$. Consequently, the $x$ component of the cutting force acting on the tool is given by the sum

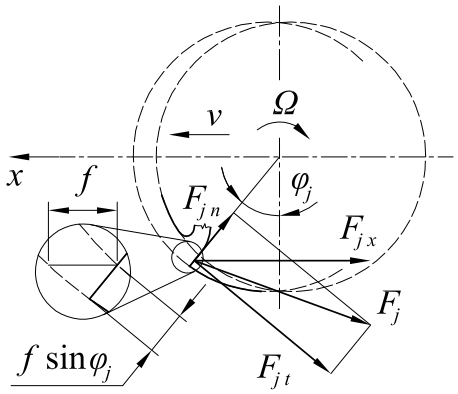


Figure 2: Cutting force components

of $F_{j\,x}$ (see equation (4)) for all $j$. Introducing the $\tau$-periodic function $q(t)$, the excitation force in equation (1) reads

$$F_x = wq(t)\left(x(t) - x(t-\tau)\right)^{x_F} \ , \tag{5}$$

where

$$q(t) = K\left(\sum_{j=1}^{z} g_j(t)\sin^{x_F}(\Omega t + j\vartheta)\left(\cos(\Omega t + j\vartheta) + 0.3\sin(\Omega t + j\vartheta)\right)\right) . \tag{6}$$

Thus, the equation of motion is the following nonautonomous nonlinear delay differential equation

$$m\ddot{x}(t) + c\dot{x}(t) + kx(t) = -wq(t)\left(x(t) - x(t-\tau)\right)^{x_F} + kvt + cv\,. \tag{7}$$

Note that the time period of $q(t)$ is equal to the time delay $\tau$.

# 3 Linearization about the unperturbed motion

Assume the tool motion in the form

$$x(t) = vt + x_p(t) + \xi(t)\,, \tag{8}$$

where $vt$ is the linear feed motion, $x_p(t) = x_p(t+\tau)$ is a $\tau$-periodic motion that can also be considered as the unperturbed, or ideal tool motion when no self-excited vibrations arise, and $\xi(t)$ is the perturbation (see Figure 1). Substitute equation (8) into equation (7)

$$m\ddot{x}_p(t) + c\dot{x}_p(t) + kx_p(t) + m\ddot{\xi}(t) + c\dot{\xi}(t) + k\xi(t) = -wq(t)\left(v\tau + \xi(t) - \xi(t-\tau)\right)^{x_F} \ . \tag{9}$$

In the ideal case, $\xi(t) \equiv 0$ and the tool moves according to $x(t) = vt + x_p(t)$. This case gives an ordinary differential equation for $x_p$

$$m\ddot{x}_p(t) + c\dot{x}_p(t) + kx_p(t) = -w(v\tau)^{x_F}q(t)\,. \tag{10}$$

Since this is a linear system with $\tau$-periodic excitation, it has a $\tau$ periodic solution, namely, the particular one. This proves the existence of the $\tau$-periodic function $x_p(t)$

and verifies equation (8). Furthermore, it can be seen that $x_p(t)$ has the same harmonics as the excitation $q(t)$. In general, this means that all the higher harmonics of the basic frequency $2\pi/\tau$ appear in $x_p(t)$.

For linear stability analysis, the variational system of equation (7) is determined about the combined linear and periodic motion $vt+x_p(t)$. Expand the nonlinear term in equation (9) into Taylor series with respect to $\xi$ and neglect the higher order terms

$$m\ddot{x}_p(t) + c\dot{x}_p(t) + kx_p(t) + m\ddot{\xi}(t) + c\dot{\xi}(t) + k\xi(t) \\ = -w(v\tau)^{x_F} q(t) - wx_F(v\tau)^{x_F-1} q(t)\left(\xi(t) - \xi(t-\tau)\right) . \quad (11)$$

Using equations (10) and (11), a linear time periodic DDE is obtained for $\xi$

$$m\ddot{\xi}(t) + c\dot{\xi}(t) + k\xi(t) = -wh(t)\left(\xi(t) - \xi(t-\tau)\right) , \quad (12)$$

where $h(t) = x_F(v\tau)^{x_F-1} q(t)$ is the specific force variation.

Equation (12) is considered as a standard linear DDE model of the milling process.

# 4 Frequencies during chatter

Chatter arises if the linear equation (12) loses stability or there is resonance in equation (10). Resonance can easily be described by the ratio of the natural frequency of the machine tool structure and the exciting frequency. This resonant case is not considered here, and only the self-excited chatter related to the loss of stability in equation (12) is considered is investigated.

The stability properties of equation (12) are determined by the infinite number of characteristic multipliers, as explained in the Introduction on the extended Floquet theory of DDEs. If $\mu = \mathrm{e}^{\lambda\tau}$ is a characteristic multiplier of equation (12), then there exists a solution in the form

$$\xi(t) = p(t)\,\mathrm{e}^{\lambda t} + \bar{p}(t)\,\mathrm{e}^{\bar{\lambda} t} , \quad (13)$$

where $p(t) = p(t+\tau)$ is $\tau$-periodic function, $\lambda$ is the so-called characteristic exponent and bar denotes complex conjugates. Equation (12) is asymptotically stable, if and only if, all the characteristic multipliers are in modulus less than one, in other words, all characteristic exponents have negative real part.

The stability analysis can be based on the determination of the relevant characteristic multiplier. There are several approximation methods to carry out this calculation [26, 22, 32]. The vibration frequencies corresponding to the relevant characteristic multiplier can be determined in the following way.

If equation (12) is at the border of stability, then there is at least one characteristic multiplier (either one real, or one complex pair) with a modulus of one. All of the other infinite number of characteristic multipliers have moduli less than one, so they are not important for chatter frequency analysis.

The critical characteristic multipliers can be located in three ways.

1. They are a complex pair located on the unit circle ($|\mu| = 1$ and $|\bar{\mu}| = 1$). This case is topologically equivalent to the Hopf bifurcation of autonomous systems and called a secondary Hopf or Neimark-Sacker bifurcation.

2. $\mu = 1$. The associated bifurcation is topologically equivalent to the saddle-node bifurcation of autonomous systems and is called a period one bifurcation.

3. $\mu = -1$. There is no topologically equivalent type of bifurcation for autonomous systems. This case is called period two, period doubling, or flip bifurcation.

It can easily be seen that the $\mu = 1$ case cannot arise in equation (12) [21, 23].

For a given $|\mu| = 1$, $\lambda = \mathrm{i}\,\omega$ is pure imaginary, where $\omega = \mathrm{Im}\,(\ln \mu)/\tau$. Essentially, the chatter frequencies are assigned by $\omega$. Since the complex exponential function is periodic, the logarithmic function is not unique in the plane of complex numbers. This raises the possibility of multiple chatter frequencies. To give a clear view of the resulting frequencies, equation (13) must be analysed.

For secondary Hopf case, the characteristic exponents are also a complex pair. Substitute $\lambda = \mathrm{i}\,\omega$ into equation (13), expand $p(t)$ into Fourier series and use trigonometrical transformations. Then equation (13) can be written in the form

$$\xi(t) = \sum_{n=-\infty}^{\infty} \left( C_n \, \mathrm{e}^{\mathrm{i}\,(\omega + n2\pi/\tau)t} + \bar{C}_n \, \mathrm{e}^{\mathrm{i}\,(-\omega + n2\pi/\tau)t} \right) , \tag{14}$$

where $C_n$'s are complex coefficients. This shows that the frequencies arising in the signal $\xi(t)$ are

$$f_H = \left\{ \pm\omega + n\frac{2\pi}{\tau} \right\} \, [\mathrm{rad/s}] = \left\{ \pm\frac{\omega}{2\pi} + n\frac{z\Omega}{60} \right\} \, [\mathrm{Hz}] , \quad n = \ldots, -1, 0, 1, \ldots , \tag{15}$$

where $\tau$ is given in [s], $\Omega$ in [rpm]. The index of $f_H$ refers to the secondary Hopf bifurcation. There are infinite number of frequencies with amplitudes corresponding to the coefficients $C_n$'s. This is in accordance with the periodic property of the complex exponential function mentioned before. Of course, only the positive values of $f_H$ have physical meaning.

For the period doubling case ($\mu = -1$), the characteristic exponent is $\lambda = (\ln(-1))/\tau$ and the frequencies can be written in the simple form of

$$f_{PD} = \left\{ \frac{\pi}{\tau} + n\frac{2\pi}{\tau} \right\} \, [\mathrm{rad/s}] = \left\{ \frac{z\Omega}{120} + n\frac{z\Omega}{60} \right\} \, [\mathrm{Hz}] , \quad n = \ldots, -1, 0, 1, \ldots , \tag{16}$$

where the index of $f_{PD}$ refers to the period doubling bifurcation.

Either the frequency set $f_H$ or $f_{PD}$ shows up during chatter. If equation (12) is stable, then these frequencies do not arise.

# 5 Other non-chatter vibration frequencies during milling

The frequencies excited during the milling operation are related to all components of $x(t)$ defined by equation (8). The term $vt$ is the linear feed motion, and it does not contain any periodicity, but the periodic motion $x_p(t)$ contains the following frequencies

$$f_{TPE} = \left\{ \frac{nz\Omega}{60} \right\} \, [\mathrm{Hz}] , \quad n = 1, 2, \ldots , \tag{17}$$

as it was shown by equation (10). The index of $f_{TPE}$ refers to the tooth pass excitation effect.

Since the damping of machine tools is small, the transient phenomena decay slowly. This results in another peak in the spectrum at the well separated lowest damped natural

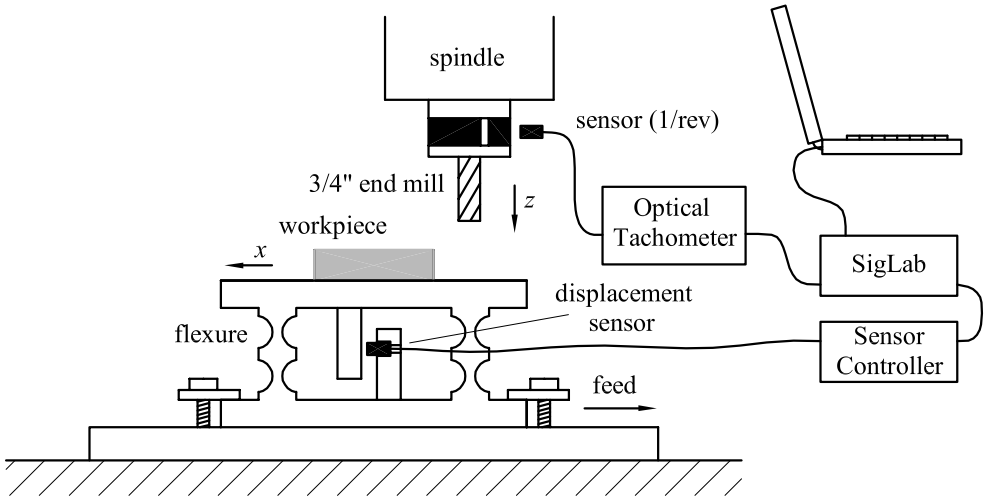


Figure 3: Scheme of the experiment

frequency $f_d = \omega_n \sqrt{1-\zeta^2}/(2\pi)$ of the machine tool structure. Here, $\omega_n = \sqrt{k/m}$ is the angular natural frequency and $\zeta = c/(2m\omega_n)$ is the relative damping factor.

The frequencies $f_{TPE}$ and $f_d$ are present in the vibration signal both for stable and unstable cutting.

# 6 Experimental verification

Milling tests were performed with an experimental flexure designed to mimic the SDOF system described above. A monolithic, uni-directional flexure was machined from aluminium and instrumented with a single non-contact, eddy current displacement transducer as shown in Figure 3. Aluminium (7075-T6) test samples of width 1/4 inch (6.35 mm) were mounted on the flexure and centrally milled by a 3/4-inch (19.05 mm) diameter carbid end mill with a single flute (the second flute was ground off to remove any effects due to asymmetry or runout). Feed was held constant: $v\tau = 0.004$ in $= 0.1016$ mm.

The stiffness of the flexure to deflections in the $x$-direction was measured to be $k = 2.2 \times 10^6$ N/m. In comparison, the values of stiffness in the orthogonal $y$- and $z$-directions were more than 20 times greater, than that in the $x$-direction. The natural frequency was experimentally determined to be $f_n = 146.8$ Hz, and the relative damping factor was $\zeta = 0.0038$, which corresponds to very light damping. Consequently, the damped natural frequency of the flexure was $f_d \approx f_n = 146.8$ Hz.

The displacement transducer output was anti-alias filtered with 500 Hz cutoff and sampled (16-bit precision, 12800 samples/sec) with SigLab 20-22A data acquisition hardware connected to a Toshiba Tecra 520 laptop computer. A periodic 1/rev pulse was obtained with the use of a laser tachometer to sense a black-white transition on the rotating tool holder (see Figure 3).

Displacement data were recorded for 15 seconds. The spectral analysis was performed using Hanning window. No averaging procedures were used. The calibration of the displacement sensor was $1.303 \times 10^{-4}$ m/V.

Theoretical stability charts and the chatter frequencies were determined through the investigation of the characteristic multipliers calculated by the semi-discretization method [32]. The infinite dimensional system (12) was approximated by a 22 dimensional discrete

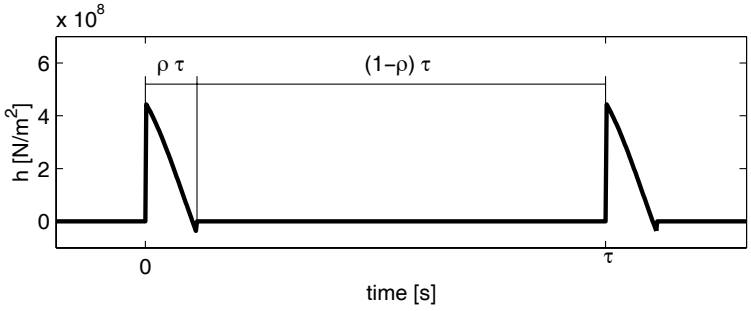


Figure 4: The specific force variation $h(t)$

system, this resulted errors less than 2% for the stability boundaries in the presented parameter domain. The execution time of one computation with fixed parameters was 0.023 s with a 400 MHz Pentium II processor. For the construction of the chart in Figure 5, an $800 \times 200$ grid was taken in the parameter plane of spindle speed and depth of cut, and the relevant characteristic multipliers were determined for each parameter points. This way, the computation time of the stability chart was about 1 hour.

For the calculations, the following experimentally identified parameters were used: $m = 2.586$ kg, $k = 2.2 \times 10^6$ N/m, $c = 18.13$ Ns/m. Based on the experimental results of Halley [30], the cutting coefficient was chosen to the reasonable value $K = 1.9 \times 10^8$ N/m$^{1+x_F}$, with $x_F = 0.8$. The value of $x_F$ is also confirmed in the book of Tlusty [29].

The relative position of the tool and the workpiece defines the specific force variation $h(t)$ from equation (12). The ratio of time spent cutting to not cutting is $\rho = 0.1082$, as it can be seen in Figure 4.

The theoretical stability chart and the corresponding chatter frequencies can be seen in Figure 5. Solid lines denote the chatter frequencies $f_H$ and $f_{PD}$. Dashed lines refer to the frequencies $f_{TPE}$ caused by the tooth pass excitation effect, and a dotted line denotes the damped natural frequency $f_d$ of the flexure.

Milling tests were carried out over a specified range of speeds and axial depths of cut. The results are presented in Figure 6, where $\circ$ denotes stable cutting, and $\times$ denotes unstable operations. The experimental data correlate with the theoretical predictions gained from this simple SDOF mechanical model. The specified parameter points A, B and C relate to constant depth of cut $w = 2$ mm and three different spindle speeds $\Omega = 3300$, 3500, and 3590 rpm, respectively. Point A is in an unstable parameter domain of Hopf type, point B is in a stable domain, and point C is in an unstable domain of period doubling type. The vertical lines raised from the corresponding parameter points of the chart intersect the frequency lines in the frequency diagram above the chart and assign the frequency sets belonging to the corresponding vibration signal of the machine tool. The symbols $\circ$, $\triangle$, $\square$ and $\bullet$ refer to the four different classes of frequency sets $f_H$, $f_{PD}$, $f_{TPE}$ and $f_d$, respectively. The same symbols also show up in Figure 8. The three power spectra are calculated from the three vibration signals presented in Figure 7 in three different forms, each: time history, sampled time history, and Poincaré (or stroboscopic) map. In the power spectra of Figure 8, the dashed lines denote the theoretical tooth pass excitation frequency and its higher harmonics. The symbols mentioned above help to identify all the various frequency sets.

For parameter point A, the theory shows that the relevant characteristic multiplier is a complex pair. The experiment confirms the theoretical expectation: the most dominant

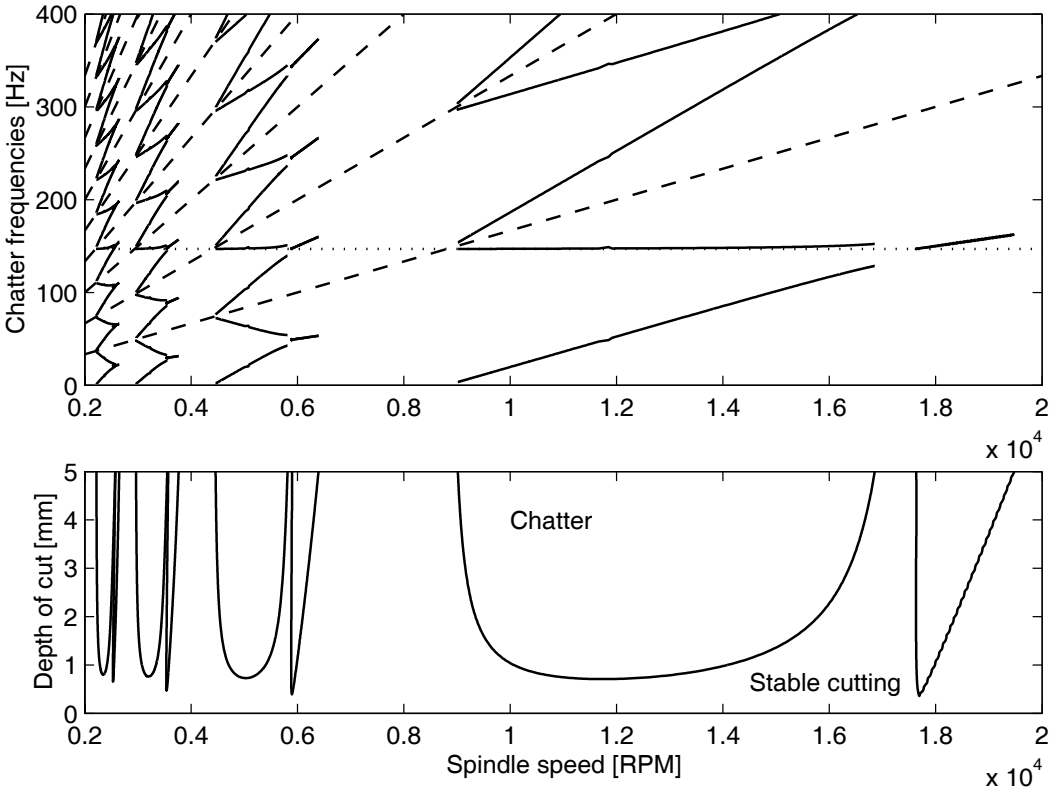


Figure 5: Theoretical stability chart and chatter frequencies

peaks in the power spectrum show up at the frequencies $f_H$, $f_{TPE}$ and $f_d$.

Cutting defined by parameter point B is stable, so only frequencies $f_{TPE}$ and $f_d$ are expected. This is also confirmed by the measurement result.

Parameter point C defines an unstable, period doubling cutting process. In this case, the most dominant peaks in the power spectrum are at the frequencies $f_{PD}$, $f_{TPE}$ and $f_d$, and clearly, it is also confirmed by the experiments.

The transition between the secondary Hopf and the period doubling case can be followed in the chatter frequency plots of Figures 5 and 6. For a secondary Hopf type chatter, there are two $f_H$-frequencies in the neighbour of each $f_{TPE}$-frequency, one below, and one above. As the spindle speed is increased, the $f_H$-frequencies move away from the $f_{TPE}$-frequencies until they meet the $f_H$-frequencies belonging to the neighbourhood of the other nearby $f_{TPE}$-frequencies, and they meet right at the middle of two $f_{TPE}$-frequencies. Above this spindle speed, the bifurcation is period doubling, that is, the $f_{PD}$-frequencies are just in the middle between two nearby $f_{TPE}$-frequencies.

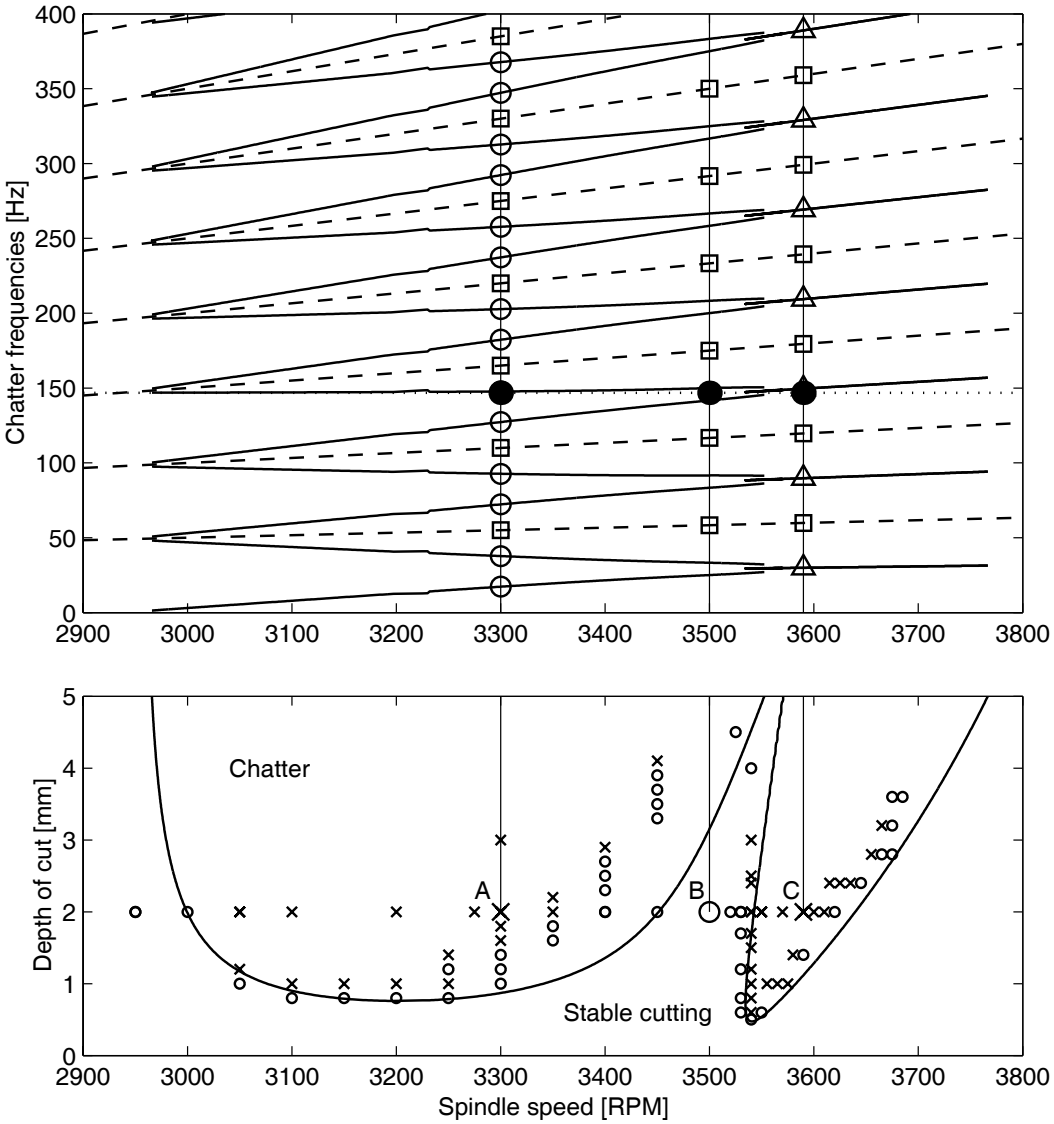


Figure 6: Theoretical stability boundaries with the corresponding vibration frequencies ($\circ$ – $f_H$, $\triangle$ – $f_{PD}$, $\square$ – $f_{TPE}$, $\bullet$ – $f_d$) and experimental results ($\circ$ - stable cutting, $\times$ - chatter)

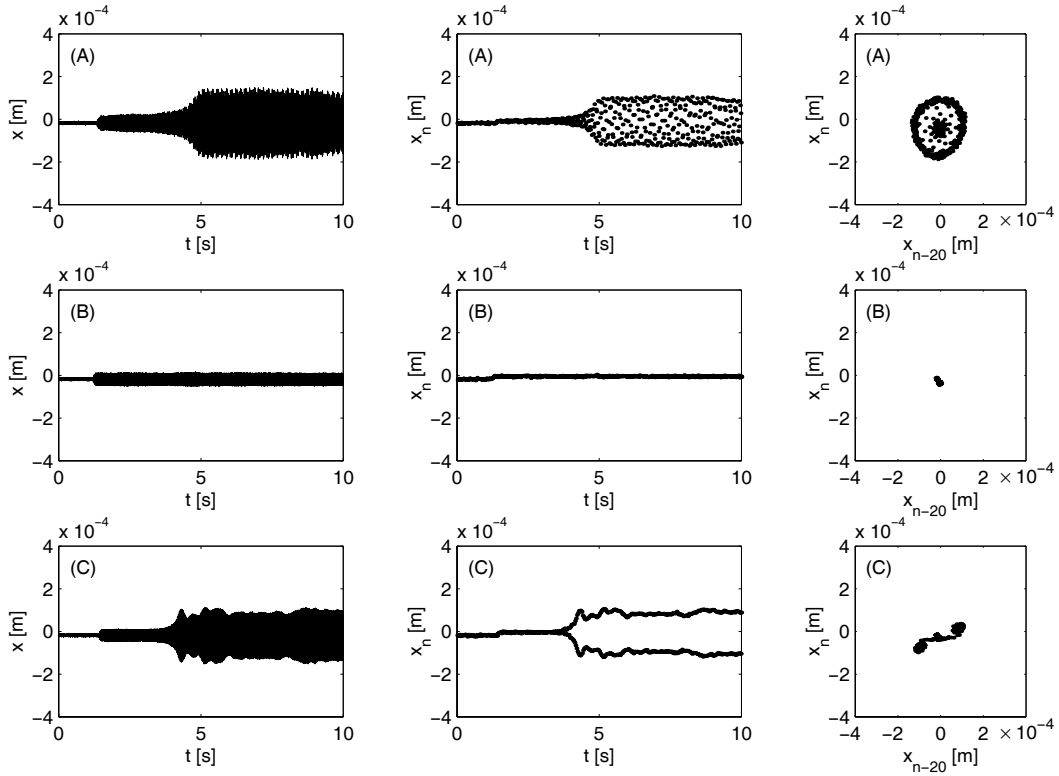


Figure 7: Continuous time histories, 1/rev sampled signals, and Poincaré sections for parameter points A, B and C

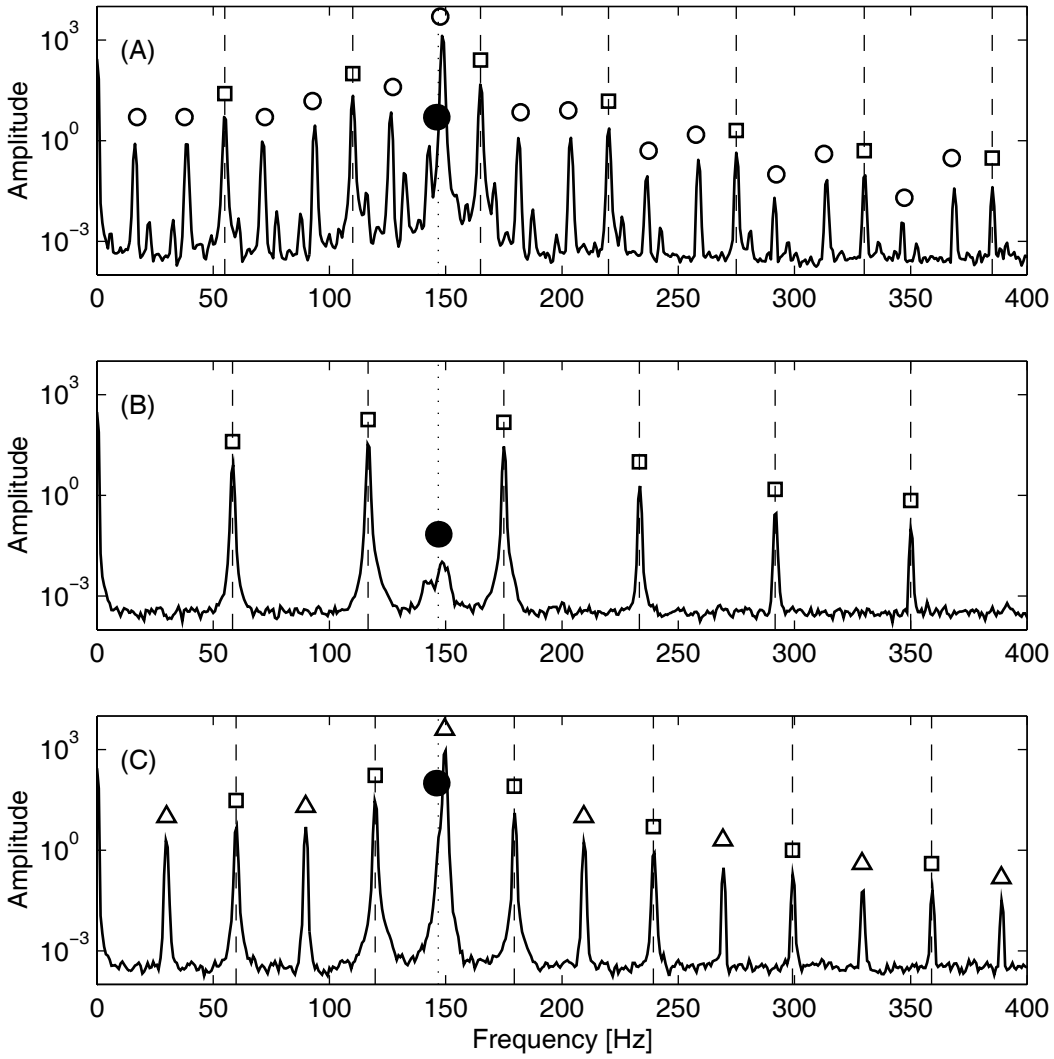


Figure 8: Power spectra for parameter points A, B and C ($\circ$ – $f_H$, $\triangle$ – $f_{PD}$, $\square$ – $f_{TPE}$, $\bullet$ – $f_d$)

# 7 Conclusions

The dynamics of the milling process is intricate due to the infinite dimensional phase space caused by the regenerative effect, and to the parametric excitation caused by the time-varying number of active teeth. Frequency analysis is also not trivial, several sets of peaks appear in the power spectra of the vibration signals.

The analytical investigation of the governing time-periodic DDEs identifies four types of frequency sets. The tooth pass excitation frequency together with its higher harmonics ($f_{TPE}$), and also the damped natural frequency ($f_d$) of the tool arise for both stable and unstable milling processes. In the unstable case, additional frequency sets occur: either Hopf type ($f_H$) or period doubling type ($f_{PD}$) frequencies. As opposed to the chatter frequencies of turning, some of the milling vibration frequencies may be smaller than the natural frequency of the tool. The results were confirmed by power spectra gained via Fourier transformation of the experimental data.

In case of high-speed milling, the period doubling type loss of stability is a recently identified mechanism of chatter in cutting processes. The clear picture of the structure of frequency components helps to distinguish between the different kinds of oscillations in intermittent cutting.

# Acknowledgements

This research was supported by the Hungarian National Science Foundation under grant no. OTKA T030762/99, the EU COST P4 action, the US National Science Foundation Grants DMI-9900108 (GOALI) and CMS-9625161 (CAREER) and the U.S. National Defense Science and Engineering Graduate Fellowship.

# References

1. F. W. Taylor 1907 *Transactions of the ASME* **28**, 31-350. On the art of cutting metals.

2. J. Tlusty, A. Polacek, C. Danek, J. Spacek 1962 *Selbsterregte Schwingungen an Werkzeugmaschinen.* Berlin: VEB Verlag Technik.

3. S. A. Tobias 1965 *Machine tool vibration.* London: Blackie.

4. F. C. Moon 1998 *Dynamics and chaos in manufacturing processes.* New York: Wiley.

5. J. E. Halley, A. M. Helvey, K. S. Smith, W. R. Winfough 1999 *Proceedings of 1999 ASME Design and Technical Conferences, Las Vegas, Nevada*, paper no. DETC99/VIB-8057 (CD-ROM). The impact of high-speed machining on the design and fabrication of aircraft components.

6. D. J. Seagalman, E. A. Butcher 2000 *Journal of Vibration and Control* **6**, 243-256. Suppression of regenerative chatter via impedance modulation.

7. A. M. Gouskov, S. A. Voronov, H. Paris, S. A. Batzer 2001 *Proceedings of the ASME 2001 Design Engineering Technical Conferences, Pittsburgh, Pennsylvania*, paper no. DETC2001/VIB-21431 (CD-ROM). Cylindrical workpiece turning using multiple-cutter tool heads.

8. G. Stépán 1989 *Retarded dynamical systems.* Harlow: Longman.

9. G. Stépán 1998 in *Dynamics and Chaos in Manufacturing Processes* (F. C. Moon, editor) 165-192. New York: Wiley. Delay-differential equation models for machine tool chatter.

10. J. Gradisek, E. Govekar, I. Grabec 1998 *Mechanical Systems and Signal Processing* **12**(6), 839-854. Time series analysis in metal cutting: chatter versus chatter-free cutting. doi: 10.1006/mssp.1998.0174

11. J. Gradisek, E. Govekar, I. Grabec 1998 *Journal of Sound and Vibration* **214**(5), 941-952. Using coarse-grained entropy rate to detect chatter in cutting. doi: 10.1006/jsvi.1998.1632

12. T. L. Schmitz, M. A. Davies, K. Medicus, J. Snyder 2001 *Annals of the CIRP* **50**(1), 263-268. Improving high-speed machining material removal rates by rapid dynamic analysis.

13. H. M. Shi, S. A. Tobias 1984 *International Journal of Machine Tool Design and Research* **24**, 45-69. Theory of finite amplitude machine tool instability.

14. G. Stépán, T. Kalmár-Nagy 1997 *Proceedings of 1997 ASME Design Engineering Technical Conferences, Sacramento, California*, paper no. DETC97/VIB-4021 (CD-ROM). Nonlinear regenerative machine tool vibration.

15. A. Halanay 1961 *Revue de Mathématiques Pures et Appliquées* **6**(4), 633-653. Stability theory of linear periodic systems with delay (in Russian).

16. J. K. Hale, S. M. V. Lunel 1993 *Introduction to functional differential equations.* New York: Springer-Verlag.

17. M. Farkas 1994 *Periodic motions.* New York: Springer-Verlag.

18. I. Minis, R. Yanushevsky 1993 *ASME Journal of Engineering for Industry* **115**, 1-8. A new theoretical approach for the prediction of machine tool chatter in milling.

19. Y. Altintas, E. Budak 1995 *Annals of the CIRP* **44**, 357-362. Analytical Prediction of stability lobes in milling.

20. T. Insperger, G. Stépán 2000 *Periodica Polytechnica* **44**(1), 47-57. Stability of the milling process.

21. M. A. Davies, J. R. Pratt, B. Dutterer, T. J. Burns 2002 *Journal of Manufacturing Science and Engineering* **124**(2), 217-225. Stability prediction for low radial immersion milling.

22. P. V. Bayly, J. E. Halley, B. P. Mann, M. A. Davies 2001 *Proceedings of the ASME 2001 Design Engineering Technical Conferences, Pittsburgh, Pennsylvania*, paper no. DETC2001/VIB-21581 (CD-ROM). Stability of interrupted cutting by temporal finite element analysis.

23. T. Insperger, G. Stépán, S. Namachchivaya 2001 *Proceedings of the ASME 2001 Design Engineering Technical Conferences, Pittsburgh, Pennsylvania*, paper no. DETC2001/VIB-21616 (CD-ROM). Comparison of the dynamics of low immersion milling and cutting with varying spindle speed.

24. B. Balachandran, M. X. Zhao 2000 *Meccanica* **35**(2), 89-109. A mechanics based model for study of dynamics of milling operations.

25. B. Balachandran 2001 *Philosophical Transactions of the Royal Society* **359**, 793-820. Non-linear dynamics of milling process.

26. T. Insperger, G. Stépán 2000 *Proceedings of the ASME Symposium on Nonlinear Dynamics and Stochastic Mechanics, Orlando, Florida,* **AMD-241**, 119-123. Stability of high-speed milling.

27. W. T. Corpus, W. J. Endres 2000 *Proceedings of the ASME Symposium on Machining Processes, Orlando, Florida,* **MED-11**, 871-878. A high-order solution for the added stability lobes in intermittent machining.

28. G. Stépán, R. Szalai 2001 *Proceedings of Dynamics and Control of Mechanical Processing, Budapest, Hungary*, 59-64. Nonlinear vibrations of highly interrupted machining.

29. J. Tlusty 2000 *Manufacturing processes and equipment.* New Yersey: Prentice Hall.

30. J. E. Halley 2000 *Stability of low radial immersion milling.* MSc Thesis, Washington University, St. Louis, Missouri.

31. B. Laczik 1986 *Vibration monitoring of cutting processes* (in Hungarian). PhD Thesis, Technical University of Budapest, Hungary.

32. T. Insperger, G. Stépán 2002 *International Journal for Numerical Methods in Engineering*, in press. Semi-discretization method for delayed systems.